

Manuscript Number: ECOLIND-10716R2

Title: From structure to function: understanding shrub encroachment in drylands using hydrological and sediment connectivity

Article Type: Research paper

Keywords: Hydrological connectivity; Sediment connectivity; Ecogeomorphic feedbacks; Shrub encroachment; Connectivity thresholds

Corresponding Author: Dr. Laura Turnbull, Ph.D.

Corresponding Author's Institution: Durham University

First Author: Laura Turnbull, Ph.D.

Order of Authors: Laura Turnbull, Ph.D.; John Wainwright

Abstract: Hydrological and sediment connectivity can help us to understand better how physical and process-based linkages govern ecogeomorphic feedbacks and identify locations where degradation is likely to be pronounced. In this study we investigate how hydrological and sediment connectivity affect ecogeomorphic feedbacks in transitional landscapes. We propose a novel approach, the Relative Connectivity Index (RCI), to quantify landscape connectivity which explicitly integrates structural measures of landscape connectivity (SC) with functional measures of hydrological and sediment connectivity (FC) that are derived from runoff and sediment-transport modelling. We use the RCI calculated for runoff (RCIH) and sediment (RCIS) to identify locations and times when functional connectivity exceeds structural connectivity thresholds - where land degradation is likely to be pronounced - and explore how these thresholds are affected by rainfall-event size and antecedent soil-moisture content. We find that there are non-linear increases in RCIH values with an increase in shrub cover, which suggest that ecogeomorphic feedbacks become more important in modifying system structure and function during late stages of shrub encroachment. Thresholds of sediment connectivity appear to be directly related to thresholds of hydrological connectivity, although rainsplash appears to be an important mechanism in creating connected sediment transport where there is no connected runoff. High RCIH values are most widely distributed for the largest (45 mm) rainfall event, whilst high RCIS values are observed to some extent across all stages of the grass to shrub transition for rainfall events as small as 10 mm. Whilst particularly large events have a low return period, they appear to be particularly instrumental in shaping ecogeomorphic feedbacks that are likely to drive catastrophic shifts in ecosystem state. The strength of the indicator approach used here is that it enables identification of regions with pronounced ecogeomorphic feedbacks, which act as potential trigger points for catastrophic shifts in ecosystem state, and thus, we demonstrate how the static limitations of existing approaches to developing connectivity indices may be overcome. The dynamic index allows the evaluation of the vulnerability or resilience of a particular system to variable driving mechanisms. The RCI can therefore be used to guide management interventions aimed at reducing

or mitigating undesirable ecosystem state change, by focussing on specific locations/regions with high RCI values, to prevent further changes in system structure and function and to maximise the provision of ecosystem services.

Response to Reviewers: In response to reviewer number 2:

Summarize the main differences between Mayor's approach and the MAHLERAN model:

- We have modified the text at lines 146-150 and 218-221 to make it clearer that we used Mahleran to model the length of runoff and sediment transport pathways that are dynamic, and compare this approximation of functional connectivity with estimates of structural connectivity - as per the Mayor approach.

L50-154 give the main rationales for the proposed indices and the paper itself. These sentences would deserve being placed earlier in the introduction, before the presentation of the indices.

- This text is now placed in the introduction, with a linking clause in the next paragraph.

L175. Could you confirm that the DTM does not integrate vegetation height. How was it produced (specifically in presence of shrubs)?

- The DTM was created by surveying the ground elevation 0.5 m resolution. We have added text at lines 187-189 to clarify this point for the reader. The DTM contains no artefacts from the vegetation height.

L181-181. I suppose the 60% value is used at the scale of the individual cell (pixel) which is 0.5 m?

- Correct. We have added "individual" into the text (now line 190) to clarify this point.

L224. Is it the percentile of cells for which values of a given RCI are above 1? If so, I don't understand the last sentence (L225-226).

- P is the percentile value at which RCIH and RCIS are ≥ 1 for the different sized rainfall events. Therefore, a lower P indicates a greater proportion of cells with RCIH and RCIS ≥ 1 , and therefore more connectivity. We have deleted the word "cumulative" from the text (now line 237) to make this point clearer.

L229. The model predicts increased connected flow pathways in presence of shrubs (L229). This is probably to be expected from the assumptions of the model itself (as to render field knowledge). If so, this should be mentioned.

- The model assumes nothing about the differences in vegetation cover. Any differences in the modelling results result from model parameterization which was based on extensive field surveys.

I am unsure to understand what differs in the interaction between topography and vegetation in the "structural computation" compared to the "functional" modelling. This is however central to understand how the RCIs behave in presence of grass or shrubs. And why there is an "observed non-linear increases in RCIH values with an increase in shrub cover" (L282).

- This difference is outlined in the methods section - the structural computation is based purely on topography and vegetation and is 'static' whereas the model (which also used vegetation and topography) also uses

dynamic rainfall and antecedent soil-moisture content to simulate runoff and sediment transport at the event timescale (as detailed in the methods), which we used to approximate functional connectivity. We have added a clarification in the methods (lines 218-221) as to why the model best represents the dynamics of functional connectivity.

Ultimately, what conceptually (and intuitively) explain why the MAHLERAN modelling predicts a stronger interaction between pathways lengths and plant type? Letting the reader intuitively grasp that would be important regarding the main message of this paper.

- as the shrub cover increases relative to other vegetation, there are a number of feedbacks, e.g. the development of splash mounds under shrubs, which tend to make the flow more convergent. These flows will reinforce infiltration on the same pathways, increase soil-moisture content, and thus reduce the importance of runoff infiltration in disrupting flow connectivity.

In response to reviewer number 2:

Summarize the main differences between Mayor's approach and the MAHLERAN model:

- We have modified the text at lines 146-150 and 218-221 to make it clearer that we used Mahleran to model the length of runoff and sediment transport pathways that are dynamic, and compare this approximation of functional connectivity with estimates of structural connectivity – as per the Mayor approach.

L150-154 give the main rationales for the proposed indices and the paper itself. These sentences would deserve being placed earlier in the introduction, before the presentation of the indices.

- This text is now placed in the introduction, with a linking clause in the next paragraph.

L175. Could you confirm that the DTM does not integrate vegetation height. How was it produced (specifically in presence of shrubs)?

- The DTM was created by surveying the ground elevation 0.5 m resolution. We have added text at lines 187-189 to clarify this point for the reader. The DTM contains no artefacts from the vegetation height.

L181-181. I suppose the 60% value is used at the scale of the individual cell (pixel) which is 0.5 m?

- Correct. We have added "individual" into the text (now line 190) to clarify this point.

L224. Is it the percentile of cells for which values of a given RCI are above 1? If so, I don't understand the last sentence (L225-226).

- P is the percentile value at which RCIH and RCIS are ≥ 1 for the different sized rainfall events. Therefore, a lower P indicates a greater proportion of cells with RCIH and RCIS ≥ 1 , and therefore more connectivity. We have deleted the word "cumulative" from the text (now line 237) to make this point clearer.

L229. The model predicts increased connected flow pathways in presence of shrubs (L229). This is probably to be expected from the assumptions of the model itself (as to render field knowledge). If so, this should be mentioned.

- The model assumes nothing about the differences in vegetation cover. Any differences in the modelling results result from model parameterization which was based on extensive field surveys.

1 I am unsure to understand what differs in the interaction between topography and vegetation in the
2 "structural computation" compared to the "functional" modelling. This is however central to
3 understand how the RCIs behave in presence of grass or shrubs. And why there is an "observed non-
4 linear increases in RCIH values with an increase in shrub cover" (L282).

5
6 - This difference is outlined in the methods section – the structural computation is based purely on
7 topography and vegetation and is 'static' whereas the model (which also used vegetation and
8 topography) also uses dynamic rainfall and antecedent soil-moisture content to simulate runoff and
9 sediment transport at the event timescale (as detailed in the methods), which we used to
10 approximate functional connectivity. We have added a clarification in the methods (lines 218-221)
11 as to why the model best represents the dynamics of functional connectivity.
12
13

14
15
16 Ultimately, what conceptually (and intuitively) explain why the MAHLERAN modelling predicts a
17 stronger interaction between pathways lengths and plant type? Letting the reader intuitively grasp
18 that would be important regarding the main message of this paper.
19

20
21 – as the shrub cover increases relative to other vegetation, there are a number of feedbacks, e.g. the
22 development of splash mounds under shrubs, which tend to make the flow more convergent. These
23 flows will reinforce infiltration on the same pathways, increase soil-moisture content, and thus
24 reduce the importance of runoff infiltration in disrupting flow connectivity.
25
26
27
28
29
30
31
32
33
34
35
36
37
38
39
40
41
42
43
44
45
46
47
48
49
50
51
52
53
54
55
56
57
58
59
60
61
62
63
64
65

Highlights

1. *FC* greatly exceeds *SC* under large rainfall events.
2. An increase in shrub cover yields non-linear increases in RCI_H values.
3. High *RCI* values show that coarse-scale *FC* overrides the smaller scale *SC* of flow paths.
4. Water and sediment connectivity have different thresholds.
5. The *RCI* can be used to identify where management interventions should be focussed.

Highlights (without abbreviations)

1. Functional connectivity exceeds structural connectivity under large rainfall events.
2. An increase in shrub cover yields non-linear increases in hydrological relative connectivity index values.
3. High hydrological relative connectivity index values show that coarse-scale functional connectivity overrides the smaller scale structural connectivity of flow paths.
4. Water and sediment connectivity have different thresholds.
5. The hydrological relative connectivity index can be used to identify where management interventions should be focussed.

From structure to function:
understanding shrub encroachment in
drylands using hydrological and
sediment connectivity

Laura Turnbull*, John Wainwright

Department of Geography, Durham University, UK

* Corresponding author. Department of Geography, Science Laboratories,
Durham University, South Rd, Durham DH1 3LE, UK

1 Abstract

2 Hydrological and sediment connectivity can help us to understand better how physical and
3 process-based linkages govern ecogeomorphic feedbacks and identify locations where
4 degradation is likely to be pronounced. In this study we investigate how hydrological and
5 sediment connectivity affect ecogeomorphic feedbacks in transitional landscapes. We
6 propose a novel approach, the *Relative Connectivity Index (RCI)*, to quantify landscape
7 connectivity which explicitly integrates structural measures of landscape connectivity (*SC*)
8 with functional measures of hydrological and sediment connectivity (*FC*) that are derived
9 from runoff and sediment-transport modelling. We use the *RCI* calculated for runoff (*RCI_H*)
10 and sediment (*RCI_S*) to identify locations and times when functional connectivity exceeds
11 structural connectivity thresholds – where land degradation is likely to be pronounced – and
12 explore how these thresholds are affected by rainfall-event size and antecedent soil-moisture
13 content. We find that there are non-linear increases in *RCI_H* values with an increase in shrub
14 cover, which suggest that ecogeomorphic feedbacks become more important in modifying
15 system structure and function during late stages of shrub encroachment. Thresholds of
16 sediment connectivity appear to be directly related to thresholds of hydrological connectivity,
17 although rainsplash appears to be an important mechanism in creating connected sediment
18 transport where there is no connected runoff. High *RCI_H* values are most widely distributed
19 for the largest (45 mm) rainfall event, whilst high *RCI_S* values are observed to some extent
20 across all stages of the grass to shrub transition for rainfall events as small as 10 mm. Whilst
21 particularly large events have a low return period, they appear to be particularly instrumental
22 in shaping ecogeomorphic feedbacks that are likely to drive catastrophic shifts in ecosystem
23 state. The strength of the indicator approach used here is that it enables identification of
24 regions with pronounced ecogeomorphic feedbacks, which act as potential trigger points for
25 catastrophic shifts in ecosystem state, and thus, we demonstrate how the static limitations of
26 existing approaches to developing connectivity indices may be overcome. The dynamic index
27 allows the evaluation of the vulnerability or resilience of a particular system to variable
28 driving mechanisms. The *RCI* can therefore be used to guide management interventions
29 aimed at reducing or mitigating undesirable ecosystem state change, by focussing on specific
30 locations/regions with high *RCI* values, to prevent further changes in system structure and
31 function and to maximise the provision of ecosystem services.

32

33 Keywords

34 Hydrological connectivity, Sediment connectivity, ecogeomorphic feedbacks, catastrophic
35 transitions; connectivity thresholds.

36

37 Highlights (with abbreviations)

38

- 39 1. *FC* greatly exceeds *SC* under large rainfall events.
- 40 2. An increase in shrub cover yields non-linear increases in RCI_H values.
- 41 3. High *RCI* values show that coarse-scale *FC* overrides the smaller scale *SC* of flow
42 paths.
- 43 4. Water and sediment connectivity have different thresholds.
- 44 5. The *RCI* can be used to identify where management interventions should be focussed.

45

46 Highlights (without abbreviations)

47

- 48 1. Functional connectivity exceeds structural connectivity under large rainfall events.
- 49 2. An increase in shrub cover yields non-linear increases in hydrological relative
50 connectivity index values.
- 51 3. High hydrological relative connectivity index values show that coarse-scale functional
52 connectivity overrides the smaller scale structural connectivity of flow paths.
- 53 4. Water and sediment connectivity have different thresholds.
- 54 5. The hydrological relative connectivity index can be used to identify where
55 management interventions should be focussed.

56

57

58

59 1. Introduction

60 In this study we use the concepts of hydrological and sediment connectivity to gain insight
61 into the location and timing of pronounced ecogeomorphic feedbacks operating in semi-arid
62 grassland and shrubland environments. Ecogeomorphic feedbacks have been identified as
63 being important dynamics that regulate the susceptibility of these systems to degradation
64 (Turnbull et al., 2012). Evidence suggests that as shrubs invade grasslands, runoff-generating
65 areas become more highly connected due to changes in soil-surface roughness and soil
66 characteristics that reduce infiltration rates (Mueller et al., 2007; Turnbull et al., 2010a,b;
67 Wainwright et al., 2000). The length of connected pathways is increasingly being recognised
68 as being an important driver of changes in system state, potentially leading to desertification
69 (e.g. Okin et al., 2009). As shrubs encroach into desert grassland, the change in connectivity
70 of flow pathways and consequential redistribution of materials – which in turn alter soil
71 characteristics and the availability of soil resources – is an important feedback mechanism by
72 which continued shrub invasion ensues (Stewart et al., 2014). These feedback processes
73 govern the coupling between structural elements of the landscape and their spatial
74 connectivity (Wainwright *et al.*, 2011), and as the length of connected pathways increase, so
75 does the scale of structural heterogeneity (e.g. Schlesinger and Pilmanis, 1998; Ludwig et al.,
76 2007). The onset and strength of these feedbacks between the connectivity of flow pathways
77 and soil properties via the redistribution of materials is likely to be a critical element
78 controlling the rate of shrub encroachment and the resilience of the shrub-invaded state.

79 Field-based experimentation has demonstrated that runoff-generating areas in
80 grassland can generate highly connected flow, but only during the most extreme rainfall
81 events that occur infrequently (e.g. Turnbull et al., 2010 a,b). In contrast, in shrubland, it has
82 been observed that runoff-generating areas become highly connected, even under relatively
83 small rainfall events. The extent to which runoff-generating areas become connected
84 determines the distance that water will flow over the land surface. This flow distance in turn
85 determines the distance over which other plant-essential resources – soil and nutrients – will
86 be redistributed (e.g. Stieglitz et al., 2003).

87 Little is still known on the specific locations and timing of ecogeomorphic feedbacks
88 within these landscapes, which is important in terms of identifying locations most susceptible
89 to degradation. These are locations where management approaches (such as modifying the
90 structural or functional connectivity of the landscape) could be targeted most effectively.

91 Here, using the concepts of hydrological and sediment connectivity, we present a novel
92 approach for the quantification of hydrological connectivity and sediment connectivity that is
93 dynamic and spatially explicit, enabling identification of locations and times when feedbacks
94 between landscape form and function (runoff and erosion) are particularly pronounced.

95 Hydrological connectivity refers to connected pathways of water transfer through a
96 system and is therefore dependent on runoff generation dynamics, the configuration of
97 runoff-generating patches, the routing of flow through a catchment and the [lack of]
98 opportunity for runoff to re-infiltrate. Sediment connectivity refers to connected pathways of
99 sediment transfers through a system and is therefore dependent on sediment detachment,
100 entrainment and connected transport through a system via wind or water. Hydrological
101 connectivity and sediment connectivity are concepts that are increasingly being referred to in
102 the fields of hydrology and geomorphology (e.g. Baartman et al., 2013; Bracken and Croke,
103 2007; Bracken et al., 2015; Turnbull et al., 2008; Wainwright et al., 2011). However,
104 application of these concepts to improve our understanding of the form and function of the
105 land surface tends to be either qualitative, or be based on runoff or erosion measurements at
106 catchments outlets. While measurements at catchment outlets are useful as they enable
107 assessment of the magnitude and duration of runoff and erosion processes, they are
108 effectively ‘black box’ as they yield no information on regions of sediment source and
109 patterns of sediment transport through the catchment. The key point to note here is that
110 hydrological connectivity and sediment connectivity metrics are only useful concepts if they
111 allow insight into land-surface processes and dynamics that measurements of landscape
112 structure, runoff or sediment flux alone cannot yield.

113 In this study, we propose a novel approach to quantifying landscape connectivity
114 which explicitly integrates structural measures of landscape connectivity with functional
115 measures. Structural measures of landscape connectivity are by definition static; they can be
116 quantified using information on the structure of the landscape surface in accordance with
117 topography or other structural features and do not account dynamically for process-form
118 linkages. Functional measures of landscape connectivity on the other hand are dynamic, and
119 vary in accordance with, for example, drivers of runoff generation such as rainfall amount
120 and antecedent soil-moisture content. These drivers of runoff in turn drive spatial and
121 temporal dynamics of erosion. The functional connectivity of a landscape will vary over very
122 short time scales, while structural connectivity is considerably less dynamic, and will change
123 in response to functional connectivity feedbacks, predominantly in response to high intensity

124 runoff events. Where the length scale of resource (water, sediment, nutrients and propagules)
125 redistribution (functional connectivity) exceeds the scale of vegetation patches (structural
126 connectivity) there is likely to be a net export of resources, and the landscape will become
127 increasingly vulnerable to change. Where the length of functional connectivity is shorter than
128 structural connectivity, resources will be retained within the landscape.

129 Our aim is to investigate where and when hydrological and sediment connectivity
130 affect ecogeomorphic feedbacks in transitional landscapes. We evaluate how dominant
131 hydrological parameters control ecogeomorphic feedbacks through changes in locations of
132 resources in the landscape, and evaluate how these can be used to develop early-warning
133 indicators for landscapes that are considered to be at risk of shrub encroachment. A classic
134 example of such a landscape is in the deserts of the US Southwest. Here, we will use data
135 collected from the Sevilleta LTER site, New Mexico, to apply the approach.

136

137 Methods

138 Previous approaches to quantifying landscape connectivity have focused on either the
139 structural connectivity of the landscape such as the connectivity of topographically lined
140 areas, or connectivity of vegetation patches (e.g. Antoine et al., 2011; Ludwig et al., 2007;
141 Mayor et al., 2008), or its functional connectivity (i.e. connectivity of the runoff response and
142 resulting flow) (e.g. Gomi et al., 2008; Jensco et al., 2009; Ocampo et al., 2006). However, a
143 more meaningful approach to quantify landscape connectivity should focus on the linkages
144 and feedbacks between the structural and functional connectivity of a landscape (Turnbull et
145 al., 2008). Here, to address feedbacks between landscape structure and function within the
146 context of connectivity, we compare functional connectivity (length of dynamic [i.e. event-
147 based] runoff and sediment transport pathways modelled using MAHLERAN) with structural
148 connectivity (estimated using field observations of vegetation cover and topography). We
149 define a dimensionless, relative connectivity index (*RCI*) as:

150

$$151 \quad RCI = \frac{FC}{SC} \quad (1)$$

152

153 where FC is a measure of functional connectivity [m] in relation to a specific process, and SC
154 is the corresponding measure of structural connectivity [m]. RCI values < 1 indicate that the
155 length of functionally connected pathways is shorter than the length of structurally connected
156 pathways. RCI values > 1 indicate that functional connectivity exceeds structural
157 connectivity. Locations and times where the $RCI > 1$ indicate when/where structural
158 thresholds are exceeded, which is important as it represents key hot spots and hot moments
159 within the landscape when structural re-organization and ecogeomorphic feedbacks are likely
160 to occur.

161 We define SC as the way in which surface characteristics (i.e. morphology, vegetation
162 and soil characteristics) are structured in a hydrologically and geomorphologically relevant
163 way, so as to facilitate the potential connected transfer of water and sediment over the
164 landscape. Two key determinants of SC (in this context) are topography, which determines
165 the direction of water flow and water-driven sediment transport, and vegetation distribution
166 as vegetation may act as a sink to which runoff from upslope areas may infiltrate, unless a
167 vegetated patch has elevated topography in which case water may be diverted around
168 vegetated patches. In arid landscapes, hydrology is one of the primary drivers of erosion, and
169 thus topography and vegetation-patch distribution are also relevant variables for defining the
170 SC of erosional processes. Thus, SC for both hydrology and erosion are conceptually and
171 quantitatively the same. Structural connectivity for each point within the landscape is thus
172 defined as the length of potentially connected flow pathways leading to that point. We use the
173 approach of Mayor et al. (2008), for each cell within a domain, the maximum length of
174 connected cells to a particular location within the landscape that does not encounter a
175 vegetation sink is calculated, thus yielding spatial estimates of structural connectivity (Figure
176 1).

177 Our method differs in two ways. First, we apply the D4, rather than the D8, steepest
178 descent flow-routing algorithm to a high-resolution (0.5 m) digital terrain model to count the
179 maximum length of topographically connected cells. This distinction is a result of the
180 structure of the model used to calculate the functional connectivity. Secondly, we used
181 millimetre-resolution aerial photography to estimate presence or absence of vegetation, which
182 was then converted to the same 0.5-m grid as the topographic data. The topographic data
183 were derived from EDM survey of the elevation of the ground surface, so do not contain
184 artefacts from the location of vegetation. Consequently, it was necessary to use a threshold to
185 define individual pixels where the vegetation cover would be significant enough to act as

186 sinks, and thus create the binary map as required by this approach. We use a threshold of 60
187 % cover, which is the mid-point in the range of observed percolation thresholds for finite
188 lattices with 4-coordination (Harel and Mouche, 2014) (Figure 2).

189 Functional connectivity (FC) in hydrological and sediment-transport contexts depends
190 not only on spatial variability of surface conditions but also on rainfall characteristics and
191 antecedent conditions. Functional connectivity can be defined for water and sediment
192 transport, based on runoff generation and flow characteristics, and sediment detachment and
193 transport processes respectively. The key point to note here is that FC will vary over space
194 and time, depending on the net interplay between antecedent conditions, rainfall event
195 characteristics and the structure of the landscape. Here, for a specific rainfall-runoff event,
196 functional hydrological connectivity and functional sediment connectivity are quantified
197 based on calculating the length of connected pathways of runoff and sediment transport to
198 each location within the study domain. These spatial measurements are seldom possible to
199 obtain through empirical observations, and thus we use spatially explicit model outputs of
200 runoff discharge and sediment transport for discrete rainfall-runoff events. The calculation
201 takes the same flow paths as defined above and follows them downslope, incrementing the
202 FC measure by the cell size for each additional cell where there continues to be flow above a
203 specified threshold. Any point where the flow drops below that threshold results in setting FC
204 to zero for that cell and restarting the increment process. For the FC of water flows (FC_H), the
205 threshold is defined as 0.249 l over an event, which equates to a 0.8 mm flow depth across
206 the 0.5-m cell, which is less than measurable in a field context; for sediment flows (FC_S) a
207 value of 0.001 kg is used, based on the lowest steady-state values for splash erosion measured
208 on a similar grassland by Parsons et al. (1994). We use an event-based runoff and erosion
209 model (MAHLERAN; Wainwright et al., 2008a) to provide spatially explicit flow and
210 sediment-transport data to calculate FC_H and FC_S . MAHLERAN has been extensively tested for
211 these and similar sites for a wide range of rainfall events and antecedent conditions, and
212 shown to produce realistic patterns as well as volumetric outputs (Turnbull et al., 2010c,
213 Wainwright et al., 2008b, c). Because MAHLERAN explicitly represents runoff infiltration and
214 uses a transport-distance approach to sediment (and adsorbed nutrient) transport, it can more
215 clearly represent the different functional dynamics that emerge in all aspects of the system
216 under variable rainfall and initial conditions than any static representation can.

217 Scenario-based analysis is carried out for four sites that are representative of different
218 stages of shrub encroachment into native desert grassland (grass, G [45 % grass]; grass-shrub,

219 G/S [39 % grass, 4 % shrub]; shrub-grass, S/G [14 % grass, 12 % shrub]; shrub, S [23 %
220 shrub]), at the Sevilleta Long Term Ecological Research site in central New Mexico USA
221 (34° 19' N, 106° 42' W; see Turnbull et al., 2010a for a full site description). Simulations are
222 carried out for four sites over a shrub-encroachment gradient that have already been
223 extensively measured and parameterized, and for which MAHLERAN has already been
224 evaluated providing confidence that it captures the dynamics of the processes at the site (see
225 Turnbull *et al.*, 2010c). The RCI is calculated for hydrological (RCI_H) and sediment
226 connectivity (RCI_S), for different antecedent soil-moisture contents (low, 3.8 %; medium,
227 10.5 %; high, 21.1 %) and for different rainfall event characteristics (Table 1) which were
228 selected based on analysis of the long-term rainfall record at the SNWR.

229 To analyse the effect of rainfall characteristics and antecedent soil-moisture content
230 on the RCI, we (i) investigate the spatial maps of connectivity metrics; (ii) explore the
231 empirical cumulative distributions (ecdf) of spatial RCI_H and RCI_S values for the four sites,
232 and then (iii) use the percentile (P) value where RCI_H or RCI_S is ≥ 1 as an overall indicator
233 of connectivity at each site. A lower P value will therefore indicate an overall higher level of
234 relative connectivity.

235

236 Results

237 The length of structurally connected flow paths increases over the transition from grassland
238 to shrubland (Figure 3). Locations where $RCI_H \geq 1$ are most widely distributed for the
239 largest (45 mm) rainfall event and to a lesser extent for the 24 mm rainfall event across all
240 plots and all antecedent soil-moisture contents (Figure 4). For the smaller rainfall events,
241 locations where the length of functionally connected hydrological pathways exceed the length
242 of structurally connected pathways are only found at the shrub (S) study site – closer to the
243 downslope boundary of this site. The ecdfs show that distribution of RCI_H values fairly
244 similar for the grass (g) and grass/shrub (G/S) site, with the G/S site showing a slightly higher
245 proportion of cells with higher RCI_H values. At the shrub/grass (S/G) site, for the 45 mm
246 rainfall event RCI_H values are much higher than for the other sites, indicating that here, the
247 length of hydrologically connected pathways greatly exceeds the length of structurally
248 connected pathways. For the 45 mm rainfall event RCI_H values are lowest at the shrub (S)
249 site, indicating that locations where functional hydrological connectivity exceeds structural
250 connectivity are less widespread than at the other sites. For the smaller rainfall events (15

251 mm, 10 mm and 5 mm), it is predominantly the shrubland site where locations with $RCI_H \geq 1$
252 are experienced.

253 The spatial patterns of RCI_S are much more pronounced across all sites than RCI_H
254 (Figure 5). Whilst the general spatial patterns of pronounced RCI_H and RCI_S are the same for
255 the 45 mm rainfall event, the strength of connectivity is much higher for sediment
256 connectivity, as indicated by the distribution of RCI_S values. The RCI_S values are also
257 relatively high for the 15 mm and 24 mm rainfall event across all plots. However, the
258 predominance of higher RCI_S values is less over the shrubland site than the others sites. For
259 the two largest rain events, overall, the grassland site has highest RCI_S values, indicating that
260 here, the length of connected sediment transport pathways is greater than the length of
261 structurally connected pathways. The RCI_S values for the shrub/grass site are similar to the
262 grassland site. For the 10mm rainfall event, RCI_S values are still relatively high at the
263 grassland/shrubland site, but comparatively lower across the other sites. For the 5 mm rainfall
264 event RCI_S values are zero in most locations indicating a lack of connected sediment
265 transport.

266 A comparison of RCI_H and RCI_S values for the 45 mm rainfall event with high
267 antecedent soil-moisture content (Figure 6) shows that whilst there is an overall positive
268 relation between the two, there is reasonable scatter (G: $R^2 = 0.74$, $p < 0.001$; G/S: $R^2 = 0.86$,
269 $p < 0.001$; S/G: $R^2 = 0.61$, $p < 0.001$; S: $R^2 = 0.89$, $p < 0.001$). Across all sites there are
270 numerous locations where RCI_H is zero and RCI_S is greater than zero. High RCI_H coupled
271 with high RCI_S values tend to occur with increasing proximity to the lower boundary of the
272 study domain, especially at the grass-dominated sites. Lower values of the RCI_H and RCI_S
273 (RCI_H and $RCI_S \sim 30$) persist at both long and short distances from the lower boundary of the
274 study domain.

275 The cumulative percentile (P) value where RCI_H or RCI_S is ≥ 1 is used as an indicator of
276 overall connectivity at each site. With an increase in event rainfall, $P(RCI_H)$ and $P(RCI_S) \geq$
277 1 decreases, indicating an overall increase in hydrological connectivity. For the grass,
278 grass/shrub and shrub/grass sites, increases in event rainfall up to 15 mm yield no changes in
279 RCI_H , followed by marginal increases in RCI_H at 24 mm and a great decrease in RCI_H at 45
280 mm event rainfall, indicating a great increase in connectivity, especially at the shrub/grass
281 site. At the shrubland site, decreases in RCI_H with an increase in event rainfall are much more
282 gradual, and less pronounced for the 45 mm rainfall event (Figure 7a). There appears to be a

283 threshold change in RCI_S between 10 and 24 mm event rainfall across low, medium and high
284 antecedent soil-moisture contents, indicating a dramatic increase in sediment connectivity
285 between these values. This threshold change is most pronounced for the sites with grass
286 cover. Similar patterns are observed when RCI_H and RCI_S are plotted against event total
287 discharge (Figure 7b).

288

289 Discussion

290 The observed non-linear increases in RCI_H values with an increase in shrub cover, most likely
291 as a function of the more constrained and convergent flow pathways that emerge, suggest that
292 ecogeomorphic feedbacks are more important with increases in shrub cover typical of the
293 later stages of shrub encroachment. These results are in line with observations from Mulga
294 landscapes in Australia where strong nonlinear behaviour of degradation processes has also
295 been observed, whereby a small shift in landscape structure can trigger a large shift in
296 ecosystem function (Moreno de las Heras et al., 2012). The widespread distribution of high
297 RCI_H values indicates high levels of functional hydrological connectivity that exceed the
298 length of structurally connected pathways. These high levels of hydrological connectivity, in
299 combination with high levels of sediment connectivity (similarly observed by the widespread
300 distribution of high RCI_S values) will drive changes in the structural connectivity of the
301 landscape, by altering the distribution and redistribution of plant-essential resources
302 (Schlesinger et al., 1996; Turnbull et al., 2010a). These structural connectivity changes also
303 alter the hydrological characteristics of the soil which will in turn affect the future
304 hydrological response of these locations to rainfall, and directly alter the structure of
305 vegetation via the erosive energy of the connected water and sediment flows (Puigdefabregas,
306 2005). A surprising observation is that values of RCI_H are lower at the shrub-dominated site
307 (which delimits the end point of the transition from grassland to shrubland) for the largest
308 rainfall event, and lower values of RCI_S for all but the smallest rainfall events. The
309 explanation for this is the level of structural connectivity is already very high, as shrublands
310 have a shrub-associated microtopography with water naturally routed over the landscape in
311 inter-shrub areas that are mostly devoid of vegetation. Therefore, high levels of hydrological
312 and sediment connectivity do not result in high RCI_H and RCI_S values. For the purpose of
313 using the RCI to identify locations where ecogeomorphic feedbacks occur, this results is
314 important, since shrublands that represent the final stage of grassland to shrubland transitions

315 are the manifestation of ecogeomorphic feedbacks that have already taken place. Therefore,
316 although there are high levels of functional hydrological and sediment connectivity, this
317 connectivity does not result in further pronounced changes to ecosystem structure. Moreover,
318 it simply maintains the current state of the landscape which is in contrast with earlier stages
319 of the grassland to shrubland transition where high levels of functional hydrological sediment
320 connectivity progressively yield changes in landscape structure. The RCI consequently
321 provides a way to assess the prevalence of cross-scale interactions, which are often an
322 important determinant of catastrophic transitions (Peters et al., 2004). RCI values > 1 indicate
323 that coarse-scale runoff/sediment transport overrides the smaller scale structural connectivity
324 of flow paths, thus exceeding the capacity of system to buffer against such extreme events. In
325 the case of the shrubland site, the scales of runoff/sediment redistribution and structural
326 connectivity of the landscape are well matched, and no threshold is exceeded.

327 Thresholds of sediment connectivity appear to be directly related to thresholds of
328 hydrological connectivity, which is not surprising considering that runoff is one of the main
329 drivers of sediment detachment and transport in this environment. The exception to this is
330 locations within each site where values of the RCI_S are greater than zero yet values of the
331 RCI_H are zero. The only plausible explanation for this observation is the role of rainsplash in
332 creating connected sediment flow and in some cases exceeds structural connectivity, even
333 where no runoff is generated.

334 An important distinction to make between the observed RCI_H and RCI_S values is that
335 high RCI_H values are most widely distributed for the largest 45 mm rainfall event, and much
336 less so for the smaller rainfall events, whilst high RCI_S values are observed to some extent
337 across all stages of the grass to shrub transition for rainfall events as small as 10 mm. Large
338 (> 10 mm) rainfall events account for as few as 20 % of the total number of rainfall events at
339 the SNWR, but contribute the majority of monsoonal precipitation – up to 66 % in wet years
340 (Petrie et al., 2014). Thus, whilst particularly large events (~ 45 mm, maximum intensity
341 211 mm h^{-1}) have a low return period (~ 50 years) (Bonnin, 2011), they are particularly
342 instrumental in driving ecogeomorphic feedbacks that are likely to drive catastrophic shifts in
343 ecosystem state. The smaller rainfall events have lower return periods (~ 5 years for the
344 24-mm rainfall event, ~ 2 years for the 15-mm rainfall event and < 1 year for the 10-mm
345 rainfall event) (Bonnin et al 2011). Thus, even though it is the most extreme events that
346 usually cause the most erosion in drylands (e.g. 5% of the rain storms cause >50 or
347 sometimes 75% of total erosion; e.g. Gonzalez-Hidalgo et al., 2007), smaller events (that still

348 have significant levels of RCI_S) are responsible for driving sediment-related ecogeomorphic
349 feedbacks due to their high frequency of occurrence. These smaller events therefore do much
350 of the ongoing 'work' in driving and maintaining functional-structural changes to the system
351 that move a system closer to the point of experiencing a catastrophic shift in ecosystem state,
352 without necessarily causing the system to 'tip' into a new and degraded shrubland state.
353 These dynamics occur at discrete locations in the landscape, as indicated by the locations of
354 high RCI_H and RCI_S values (Figures 4 and 5). Whilst the initial effects are localised, the
355 longer term implications of these changes will be more widespread. High levels of RCI_H and
356 RCI_S will result in localised increases in the structural connectivity of the landscape. For
357 instance, pronounced step and riser topography in grassland impedes flow connectivity
358 (Parsons et al., 1997), but under extreme conditions, concentrated runoff can cut through
359 these structural microtopographic barriers and modify the structural connectivity of the
360 landscape. These increases in structural connectivity will in turn facilitate future increases in
361 the functional hydrological and sediment connectivity which impact the structural
362 connectivity in downslope/adjacent locations causing further increases in RCI_H and RCI_S
363 elsewhere within the landscape. Hence, the effects of increases in ecogeomorphic feedbacks
364 at specific points within the landscape will eventually spread across the entire landscape
365 driving widespread change.

366 The observation that some of the higher values of the RCI_H and RCI_S are located
367 nearer to lower boundary of the study site indicates the partial significance of landscape
368 position in controlling locations where ecogeomorphic thresholds might be exceeded. With
369 an increase in contributing area, it becomes more likely for the length of hydrologically
370 connected flow pathways to exceed the length of structurally connected pathways, therefore
371 increasing RCI_H . These increases in RCI_H drive increases in the sediment detachment and
372 transport capacity of the flow, therefore increasing the propensity for the length of pathways
373 of connected sediment transport to exceed the length of structurally connected pathways.
374 Nevertheless, results do indicate that there are locations, irrespective of distance to the lower
375 boundary of the study domain, where the RCI_H and RCI_S are high, indicating the additional
376 importance of local ecogeomorphic characteristics, including vegetation cover, local
377 topography, and soil hydrological and erosion characteristics.

378 In landscape connectivity studies, connectivity analysis often forms the basis for
379 management actions (Rudnick et al., 2012), and similarly, in the context of shrub
380 encroachment into grasslands, quantifying changes in connectivity can not only help us

381 understand key processes and feedbacks, but can also provide a framework to evaluate
382 strategies for mitigating undesirable changes in system state (Okin et al., 2009). The indicator
383 approach used in this study similarly enables us identify regions with pronounced
384 ecogeomorphic feedbacks which act as potential trigger points for catastrophic shifts in
385 ecosystem state (Figure 8). The large patches shown in Figure 9 are where shrubs are located,
386 and these will be more resilient to high connectivity than smaller patches. Over time, these
387 locations will continue to evolve, in line with the ecogeomorphic structural-functional
388 evolution of the system (Figure 9). Management interventions aimed at reducing or
389 mitigating undesirable ecosystem state change should thus be focussed on these specific
390 locations as a starting point, to prevent further changes in system structure and function and
391 to maximise the provision of ecosystem services. In rangelands, for example, the *RCI* might
392 be used to identify regions where grazing should be excluded, or where vegetation restoration
393 measures should be focussed restore a system to a less vulnerable state. What is clear from
394 this approach is that to usefully identify and manage undesirable changes in ecosystem state,
395 the evolution of system structure and function must be accounted for, and strategies be
396 updated/located accordingly.

397 The magnitude of the *RCI* (i.e. the extent to which functional connectivity exceeds
398 structural connectivity) is an important consideration in designing suitable
399 interventions/remediation strategies. For instance, areas where the length of functionally
400 connected pathways greatly exceeds the length of structurally connected pathways may
401 require larger-scale interventions because of inertia that a small-scale manipulation is less
402 likely to overcome, and thus, the scale of the potential remediation should match scale of
403 connectivity (Okin et al., 2009), or the extent to which functional connectivity exceeds
404 structural connectivity.

405 We have demonstrated the potential utility of this approach at the hillslope scale. It
406 could also, however, be applied at larger and coarser spatial scales, with the approach being
407 used to identify key regions within a watershed where the $RCI > 1$. In this context, rather than
408 using the approach to identify specific points, it could be used to identify key regions where
409 management interventions should be focussed. For using connectivity indicators to inform
410 management actions, the approach presented here is advantageous over other approaches in
411 hydrology and geomorphology that tend to be focussed on quantifying the connectivity of
412 flows to the catchment outlet (e.g. Antoine et al., 2009) which do not allow specific locations
413 for management interventions to be identified.

414

415 Conclusions

416 To move from conceptual approaches of the links between structural and functional
417 connectivity and how they drive ecogeomorphic processes (Bracken et al., 2015; Lexartza-
418 Artza and Wainwright, 2009; Turnbull et al., 2008; Wainwright et al., 2011) to a practical
419 application, we have produced an indicator accounting for both aspects of connectivity. By
420 quantifying functional connectivity via modelling, we have been able to account for the
421 dynamically changing conditions of connectivity that are very difficult to capture using
422 monitoring approaches. In so doing, we demonstrate how the static limitations of existing
423 approaches to developing connectivity indices may be overcome. Furthermore, the dynamic
424 index allows the evaluation of the vulnerability or resilience of a particular system to variable
425 driving mechanisms. Dryland environments are inherently characterized by climate
426 variability, and therefore it is particularly relevant that our indicator approach enables the
427 evaluation of system resilience to internal variations. Both climate change and increasing
428 human pressure are also significant sources of external variation in these environments, and
429 these may be accounted for explicitly in our indicator approach, through the direct effect of
430 human pressures on modifying structural connectivity, or by climate-change effects on both
431 functional connectivity and structural connectivity.

432 Using the different behaviours of the RCI_H and RCI_S , we demonstrate that water and sediment
433 connectivity have different thresholds. To date, there has been a focus on hydrological
434 connectivity in studies of dryland dynamics, as it is easier to measure. The different
435 thresholds imply that there are different timescales of response of water and sediment, as well
436 as different spatial scales. By focussing on only one type of connectivity, the detail of
437 catastrophic shifts may be missed, given that other feedbacks are inherent in dryland
438 degradation, such as nutrient and seed-bank depletion (Stewart et al., 2014; Moreno-de las
439 Heras et al., 2016), which are also driven in non-linear ways by water and sediment fluxes.

440 Mitigating undesirable changes in landscape structure and function must be underpinned by
441 an understanding of the system complexities and their spatial and temporal scales using
442 broader concepts of connectivity studies. This study has demonstrated how a connectivity
443 indicator can be used to understand these complexities and identify critical locations where
444 management interventions or restoration efforts should be focussed to mitigate undesirable
445 changes that lead to catastrophic vegetation transitions.

446

447

448 References

- 449 Antoine, M., Jacaux, M., Bielders, C.L. 2009. What indicators can capture runoff-relevant connectivity
450 properties of the microtopography at the plot scale? *Advances in Water resources*. 32: 1297 – 1310.
451
- 452 Antoine, M., Javaux, M., Biielders, C.L., 2011. Integrating subgrid connectivity properties
453 of the micro-topography in distributed runoff models, at the interrill scale. *Journal of Hydrology*.
454 403, 213–223.
455
- 456 Baartman, J., Masselink, R., Keesstra, S.D., Temme, A. 2013. Linking landscape morphological
457 complexity and sediment connectivity. *Earth Surface Processes and Landforms*. 38: 1457 – 1471.
458
- 459 Bonnin, G.M., Martin, D., Lin, T., Parzybok, T., Yekta, M., Riley, D. 2011. Precipitation-Frequency
460 Atlas of the United States. NOAA Atlas 14 Volume 1 Version 5.0.
- 461 Bracken, L.J. & Croke, J. 2007. The concept of hydrological connectivity and its contribution to
462 understanding runoff-dominated geomorphic systems. *Hydrological Processes*. 21:1749-1763.
- 463 Bracken, L.J., Turnbull, L., Wainwright, J., Bogaart, P. 2015. Sediment connectivity: a framework for
464 understanding sediment transfer at multiple scales. *Earth Surface Processes and Landforms*. 40:177-
465 188. DOI:10.1002/esp.3635
- 466 Gomi, T., Sidle, R.C., Miyata, S., Kosugi, K., Onda, T. (2008) Dynamic runoff connectivity of
467 overland flow on steep forested hillslopes: Scale effects and runoff transfer. *Water Resources*
468 *Research*. 44: W08411.
- 469• Gonzalez-Hidalgo, J, C., Monne, J.L.C, de Luis, M. (2007) A review of daily soil erosion in Western
470 Mediterranean areas. *Catena*. 71: 193-199.
471
- 472 Harel, M-A., Mouche, E., 2014. Is the connectivity function a good indicator of soil infiltrability
473 distribution and runoff flow dimension? *Earth Surface Processes and Landforms*. 39: 1514–1525.
- 474 Jencso, K.G., McGlynn, B.L., Gooseff, M.N., Wondzell, S.M., Bencala, K.E., Marshall, L.A., 2009.
475 Hydrologic connectivity between landscapes and streams: transferring reach and plot-scale
476 understanding to the catchment scale. *Water Resources Research*. 45: W04428
- 477 Lexartza-Artza, I., Wainwright, J., 2009. Hydrological connectivity: linking concepts with practical
478 implications. *Catena*. 79, 146–152.

- 479 Ludwig, J.A., Bastin, G.N., Chewings, V.H. et al (2007) Leakiness: a new index for monitoring the
480 health of arid and semi-arid landscapes using remotely sensed vegetation cover and elevation data.
481 Ecological indicators. 7: 442 – 254.
- 482 Mayor, A.G., Bautista, S., Small, E.E., Dixon, M., Bellot, J. 2008. Measurement of the connectivity of
483 runoff source areas as determined by vegetation pattern and topography: A tool for assessing potential
484 water and soil losses in drylands. Water Resources Research. 44: DOI: 10.1029/2007WR006367
- 485 Moreno de las Heras, M., Saco, P.M., Willgoose, G.R., Tongway, D.J. (2012) Variations in
486 hydrological connectivity of Australian semiarid landscapes indicate abrupt changes in rainfall use
487 efficiency of vegetation. Journal of Geophysical research. 117: G03009.
- 488 Moreno de las Heras, M., Turnbull, L., Wainwright, J. (2016) Seed-bank structure and plant-
489 recruitment conditions regulate the dynamics of a grassland-shrubland Chihuahuan ecotone. Ecology.
490 97: 2303 – 2318.
- 491 Mueller, E.N., Wainwright, J., Parsons, A.J. (2007) Impact of connectivity on the modelling of
492 overland flow within semiarid shrubland environments. Water resources research. 43: W09412.
- 493 Ocampo, C.J., Sivapalan, M., Oldham, C., 2006. Hydrological connectivity of uplandriparian zones in
494 agricultural catchments: Implications for runoff generation and nitrate transport. J. Hydrol. 331, 643–
495 658.
- 496 Okin, G.S., Parsons, A.J., Wainwright, J., Herrick, J.E., Bestelmeyer, B.T., Peters, D.C., Fredrickson,
497 E.L. (2009) Do changes in connectivity explain desertification? Bioscience. 59: 237 – 244.
- 498 Parsons, A.J., Abrahams, A.D., Wainwright, J. 1994. Rainsplash and erosion rates in an interrill area
499 on semi-arid grassland, southern Arizona, Catena 22: 215–226. Peters, D. P., Pielke, R.A.,
500 Bestelmeyer, B.T., Allen, C.D., Munson-McGee, S., Havstad, K.M. (2004) Cross-scale interactions,
501 nonlinearities, and forecasting catastrophic events. Proceedings of the National Academy of Sciences.
502 101: 15130 – 15135.
- 503 Parsons, A.J., Wainwright, J., Abrahams, A.D. and Simanton, J.R. 1997. Distributed dynamic
504 modelling of interrill overland flow. Hydrological processes. 11: 1833 – 1859.
- 505 Petrie, M.D., Collins, S.L., Gutzler D.S., Moore, D.M. 2014. Regional trends and local variability in
506 monsoon precipitation in the northern Chihuahuan Desert, USA. Journal of Arid Environments. 13:
507 63 – 70.
- 508 Puigdefabregas J (2005) The role of vegetation patterns in structuring runoff and sediment fluxes in
509 drylands. Earth Surface Processes and Landforms. 30: 133 – 147.

- 510 Rudnick, D., Ryan, S.J., Beier, P., Cushman, S.A., Dieffenbach, F., Epps, C.W., Gerber, L.R.,
511 Hartter, J., Jenness, J.S., Kintsch, J., Merenlender, A.M., Perkl, R.M., Preziosi, D.V., Trombulak, S.C.
512 (2012) The role of landscape connectivity in planning and implementing conservation and restoration
513 priorities. *Issues in Ecology*. Report No. 16. Ecological Society of America. Washington, D.C.
- 514 Schlesinger, W.H. and Pilmanis, A.M. (1998) Plant-soil interactions in deserts. *Biogeochemistry*.
515 42: 169 – 187.
- 516 Schlesinger, W.H., Raikes, J.A., Hartley, A.E. and Cross, A.F. (1996) On the spatial pattern of soil
517 nutrients in desert ecosystems. *Ecology*. 77: 364 – 374.
- 518 Stewart, J., Parsons, A.J., Wainwright, J. et al (2014) Modeling emergent patterns of dynamic desert
519 ecosystems. *Ecological Monographs*. 84: 373 – 410.
- 520 Stieglitz, M., Shaman, J., McNamara, J., Engel, V., Shanley, J., Kling, G.W. (2003) An approach to
521 understanding hydrologic connectivity on the hillslope and the implications for nutrient transport.
522 *Global Biogeochemical Cycles*, 17: 1105.
- 523 Turnbull, L., Wainwright, J. & Brazier, R.E. 2008. A conceptual framework for understanding semi-
524 arid land degradation: ecohydrological interactions across multiple-space and time scales.
525 *Ecohydrology*. 1:23-34.
- 526 Turnbull, L., Wainwright, J., Brazier, R.E. & Bol, R. 2010a. Biotic and Abiotic Changes in Ecosystem
527 Structure over a Shrub-Encroachment Gradient in the Southwestern USA. *Ecosystems*. 13:1239-1255.
- 528 Turnbull, L., Wainwright, J. & Brazier, R.E. 2010b Changes in hydrology and erosion over a
529 transition from grassland to shrubland. *Hydrological Processes*. 24:393-414.
- 530 Turnbull, L., Wainwright, J. & Brazier, R.E. 2010c. Hydrology, erosion and nutrient transfers over a
531 transition from semi-arid grassland to shrubland in the South-Western USA: A modelling assessment.
532 *Journal of Hydrology*. 388:258-272.
- 533 Turnbull, L., Wilcox, B.P., Belnap, J., Ravi, S., D'Odorico, P., Childers, D.L., Gwenzi, W., Okin,
534 G.S., Wainwright, J., Caylor, K.K. & Sankey, T. 2012. Understanding the role of ecohydrological
535 feedbacks in ecosystem state change in drylands. *Ecohydrology*. 5:174-183.
- 536 Wainwright, J., Parsons, A.J., Abrahams A.D. (2000) Plot-scale studies of vegetation, overland flow
537 and erosion interactions: case studies from Arizona and New Mexico. *Hydrological Processes*. 14:
538 2921 – 2943.
- 539 Wainwright, J., Parsons, A.J., Muller, E.N., Brazier, R.E., Powell, D.M. & Fenti, B. 2008a. A
540 transport-distance approach to scaling erosion rates: 1. Background and model development. *Earth
541 Surface Processes and Landforms*. 33:813-826.

542 Wainwright, J., Parsons, A.J., Müller, E.N., Brazier, R.E., Powell, D.M., Fenti, B. 2008b. A transport-
543 distance approach to scaling erosion rates: 2. Sensitivity and evaluation of Mahleran. *Earth Surface*
544 *Processes and Landforms*.33: 962 – 984.

545 Wainwright, J., Parsons, A.J., Muller, E.N., Brazier, R.E., Powell, D.M. & Fenti, B. 2008b. A
546 transport-distance approach to scaling erosion rates: 3. Evaluating scaling characteristics of
547 MAHLERAN. *Earth Surface Processes and Landforms*. 33: 1113 – 1128.

548 Wainwright, J., Turnbull, L., Ibrahim, T.G., Lexartza-Artza, I., Thomton, S.F. & Brazier, R.E. 2011.
549 Linking Environmental Régimes, Space and Time: Interpretations of Structural and Functional
550 Connectivity. *Geomorphology*. 126:387-404.

551

Table 1. Rainfall event characteristics for which RCI_H and RCI_S are calculated. Event rainfall total (mm)	Rainfall intensity (mm hr^{-1})
5	48
10	61
15	76
24	91
45	211

552

553

554 List of tables

555 **Table 1.** Rainfall event characteristics for which RCI_H and RCI_S are calculated.

556 List of figures

557 **Figure 1.** Aerial imagery used to calculate % vegetation cover (left); resulting % vegetation cover
 558 map (centre); and topographically defined maximum flow path length (no. cells; right).

559 **Figure 2.** Sensitivity of structural connectivity metric (showing length of connected pathways (no.
 560 cells)) to vegetation cover thresholds used to define runoff sink cells.

561 **Figure 3.** Spatial plots of SC, based on the topographically defined maximum flow path length and
 562 structural disconnectivity where vegetation cover $\geq 60\%$.

563 **Figure 4.** Spatial plots of RCI_H for different total rainfall event size (45 mm, 24 mm, 15 mm, 10 mm
 564 and 5 mm), for high soil-moisture content (left) and associated empirical cumulative distribution
 565 function of spatial RCI_H values (right).

566 **Figure 5.** Spatial plots of RCI_S for different total rainfall event size (45 mm, 24 mm, 15 mm, 10 mm
 567 and 5 mm), for high antecedent soil-moisture content (left) and associated empirical cumulative
 568 distribution function of spatial RCI_S values (right).

569 **Figure 6.** Relation between RCI_H and RCI_S for the 45 mm rainfall event for high antecedent soil-
 570 moisture content. Points are shaded according to distance (m) from the lower boundary of the study
 571 domain.

572 **Figure 7.** Percentile value (P) at which RCI_H and RCI_S are ≥ 1 (i.e. connected) for (a) the different
 573 sized rainfall events and (b) the associated total discharge generated at the lower boundary of the
 574 study domain, plotted for low, medium and high soil-moisture content.

575 **Figure 8.** Locations at each of the study sites where $RCI_H \geq 1$ overlap with locations where
576 vegetation cover $\geq 60\%$ cover causing structural disconnectivity (for the 45 mm rainfall event with
577 high antecedent soil-moisture content). These are the locations where pronounced ecogeomorphic
578 feedbacks will occur.

579 **Figure 9.** Conceptual model showing how structural-functional feedbacks drive changes in ecosystem
580 state following an initial disturbance, due to pronounced ecogeomorphic feedbacks (*PEF*) occurring at
581 specific locations within the landscape that can be identified using the $RCI_{H,S}$. Ecogeomorphic
582 feedbacks occurring at these locations will drive changes in system structure and function with effects
583 cascading to adjacent/downslope locations. Interventions targeted at these locations with *PEF* may
584 provide an opportunity to halt further ecogeomorphic feedbacks and prevent a catastrophic transition
585 to a final shrub-dominated state.

586

587

*Manuscript (revision changes marked)

[Click here to download Manuscript \(revision changes marked\): From structure to function in plant evolution.pdf](#)

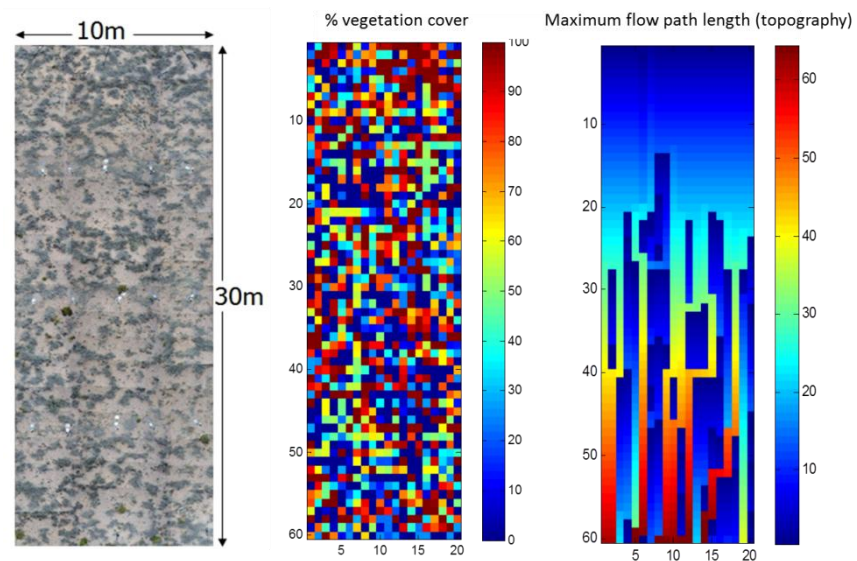


Figure 1. Aerial imagery used to calculate % vegetation cover (left); resulting % vegetation cover map (centre); and topographically defined maximum flow path length (no. cells; right).

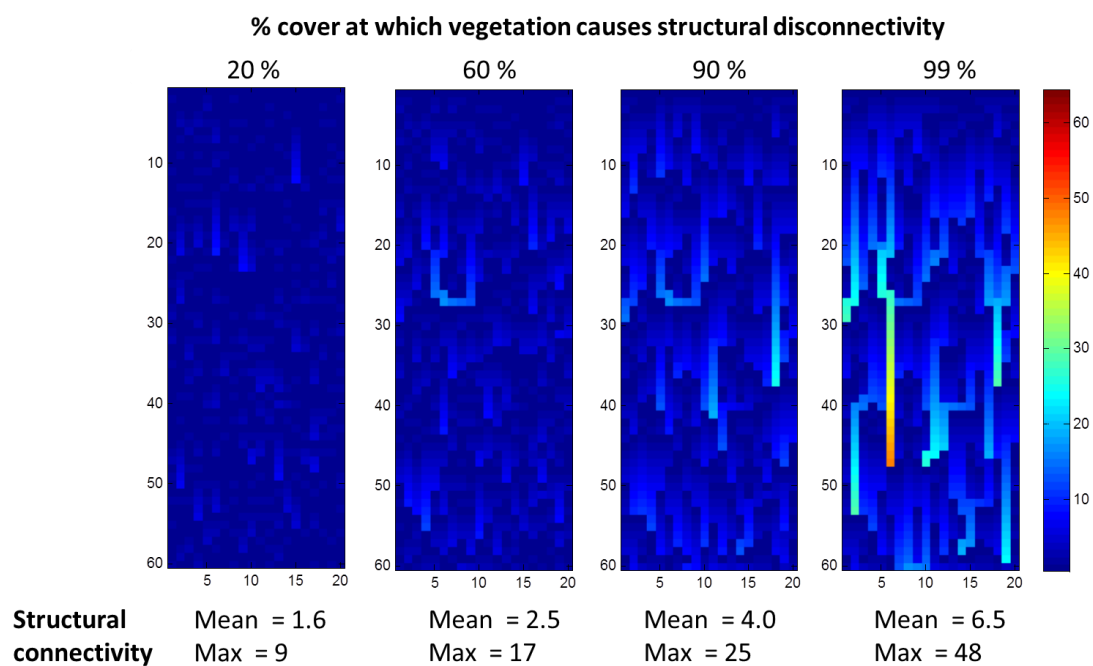


Figure 2. Sensitivity of structural connectivity metric (showing length of connected pathways (no. cells)) to vegetation cover thresholds used to define runoff sink cells.

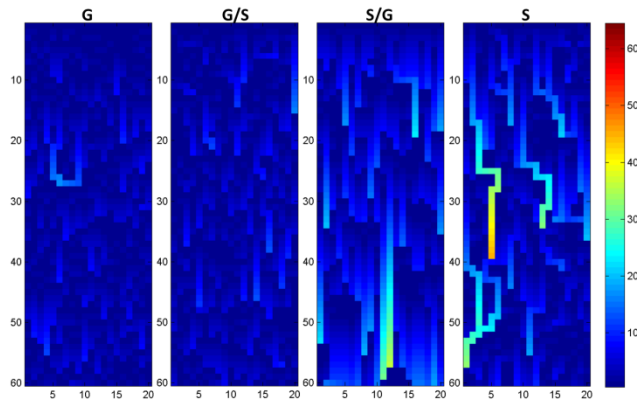


Figure 3. Spatial plots of SC, based on the topographically defined maximum flow path length and structural disconnectivity where vegetation cover $\geq 60\%$.

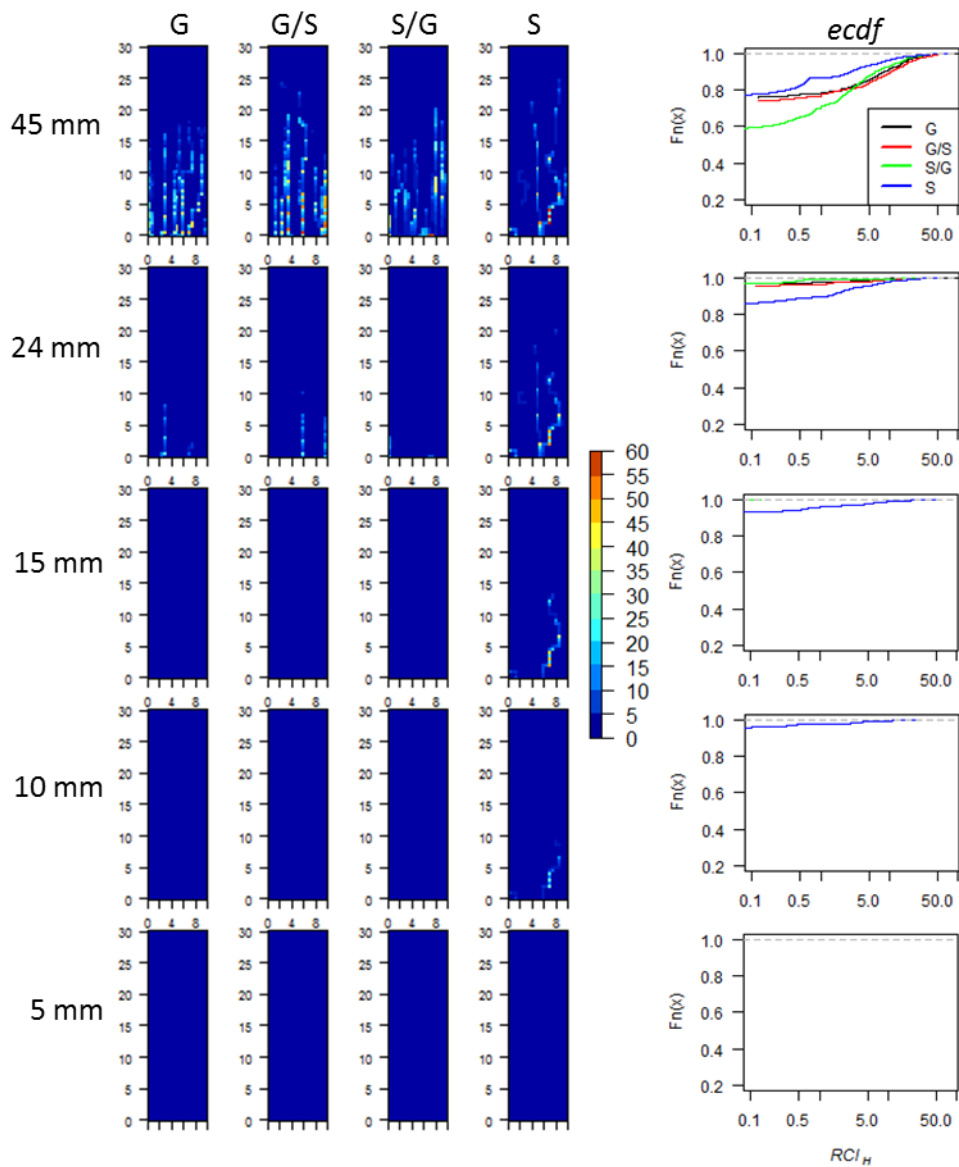


Figure 4. Spatial plots of RCI_H for different total rainfall event size (45 mm, 24 mm, 15 mm, 10 mm and 5 mm), for high soil-moisture content (left) and associated empirical cumulative distribution function of spatial RCI_H values (right).

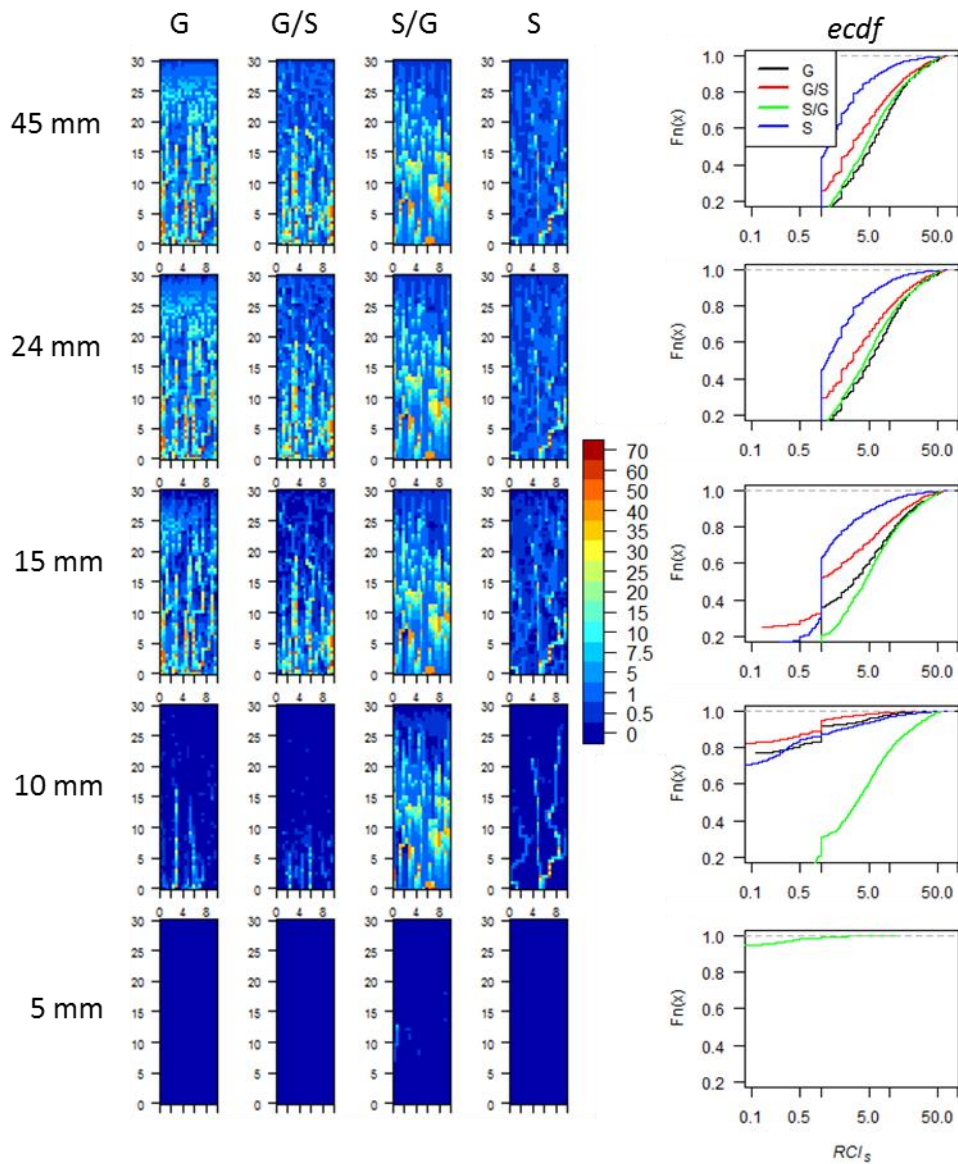


Figure 5. Spatial plots of RCI_5 for different total rainfall event size (45 mm, 24 mm, 15 mm, 10 mm and 5 mm), for high antecedent soil-moisture content (left) and associated empirical cumulative distribution function of spatial RCI_5 values (right).

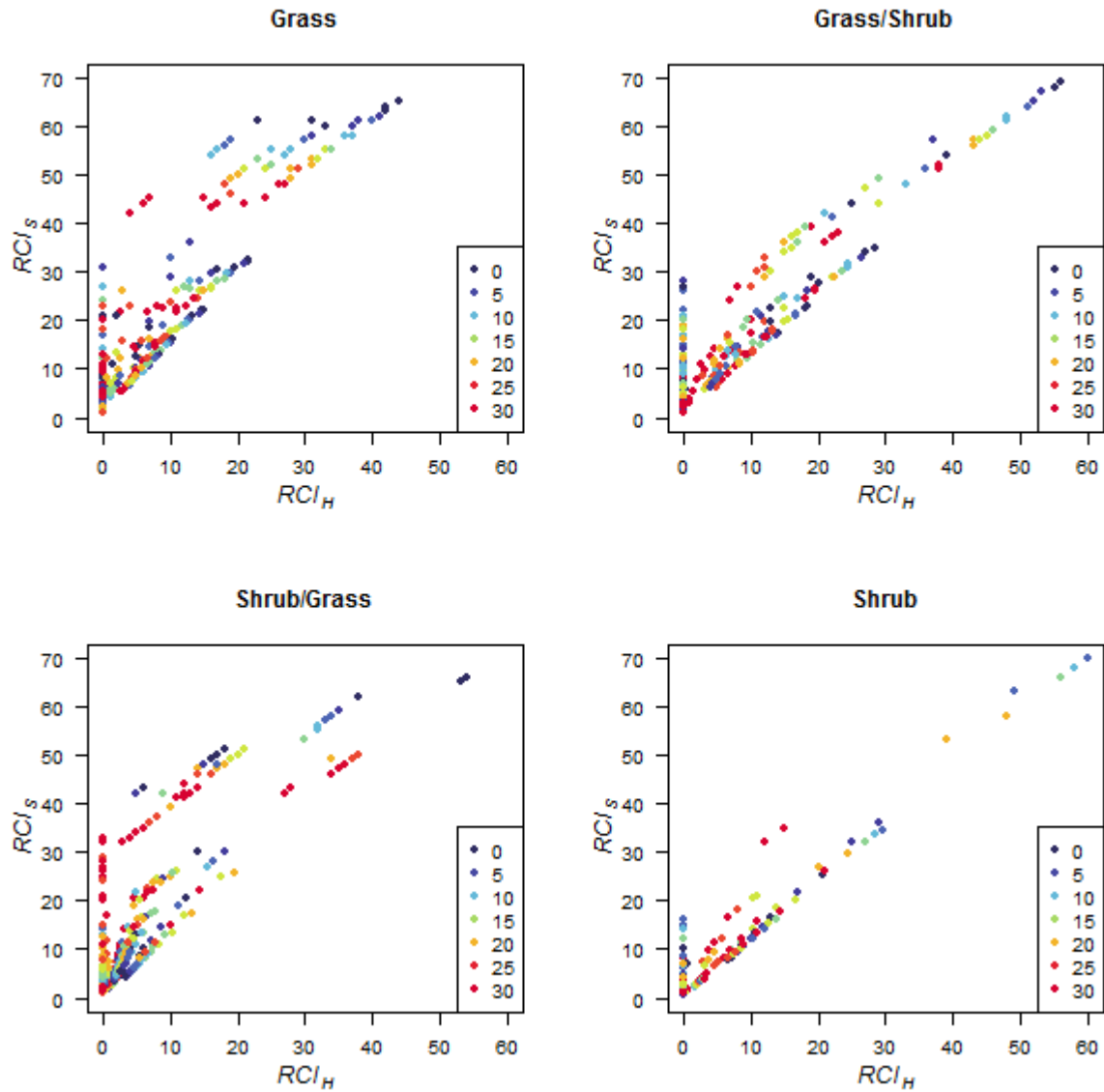


Figure 6. Relation between RCI_H and RCI_S for the 45 mm rainfall event for high antecedent soil-moisture content. Points are shaded according to distance (m) from the lower boundary of the study domain.

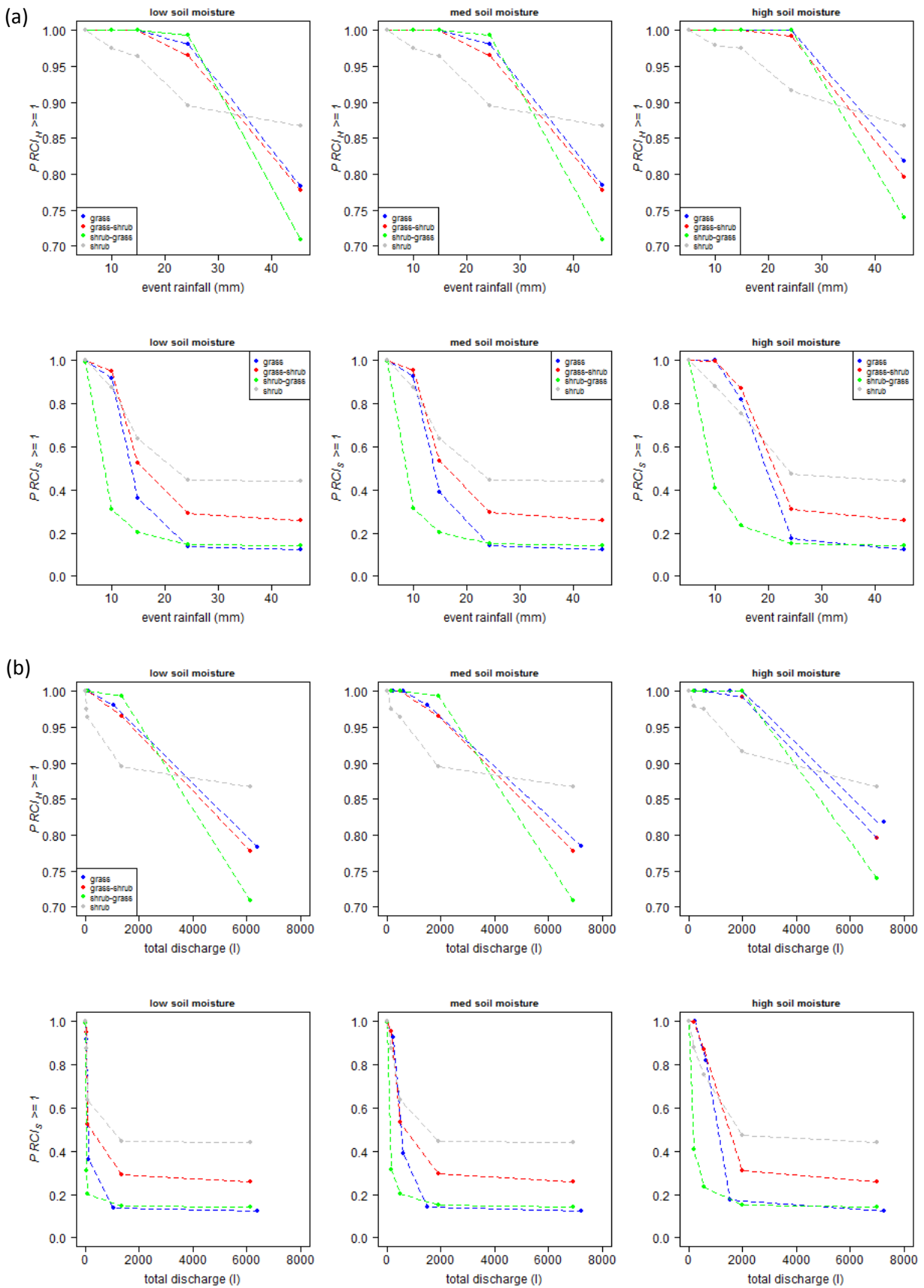


Figure 7. Percentile value (P) at which RCI_H and RCI_S are ≥ 1 (i.e. connected) for (a) the different sized rainfall events and (b) the associated total discharge generated at the lower boundary of the study domain, plotted for low, medium and high soil-moisture content.

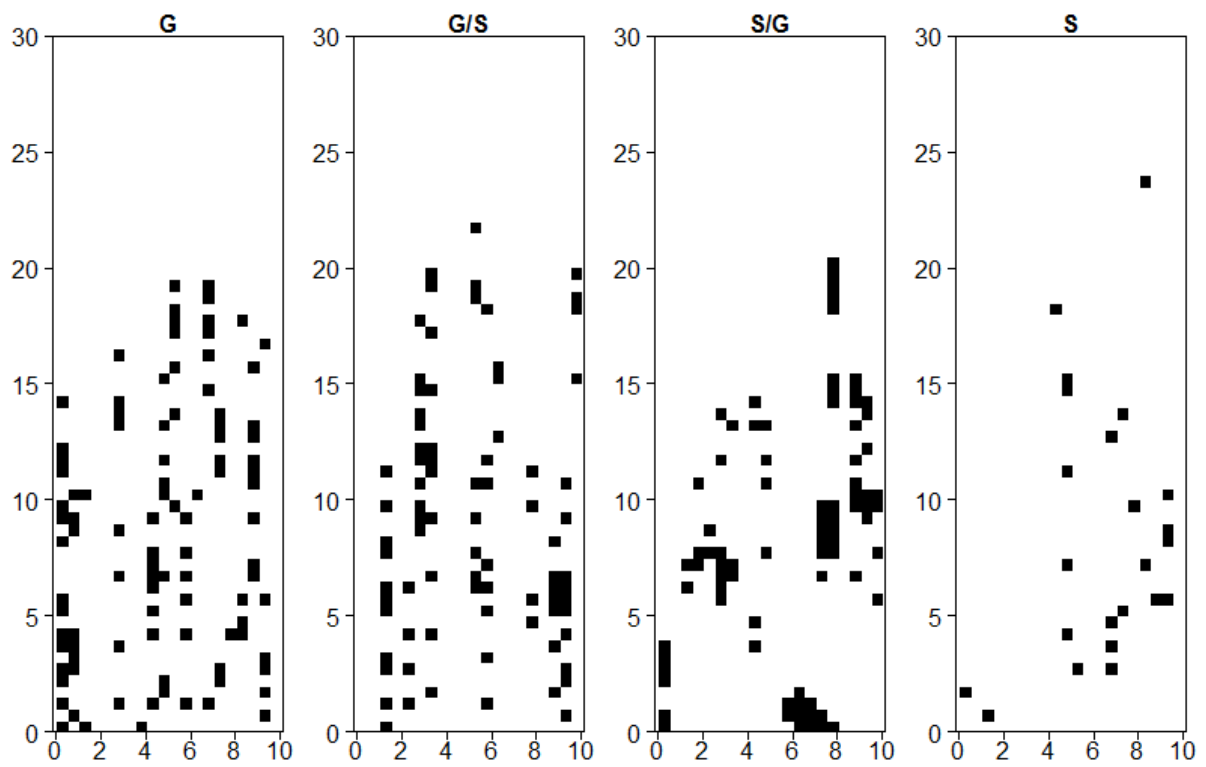


Figure 8. Locations at each of the study sites where $RCI_H \geq 1$ overlap with locations where vegetation cover $\geq 60\%$ cover causing structural disconnection (for the 45 mm rainfall event with high antecedent soil-moisture content). These are the locations where pronounced ecogeomorphic feedbacks will occur.

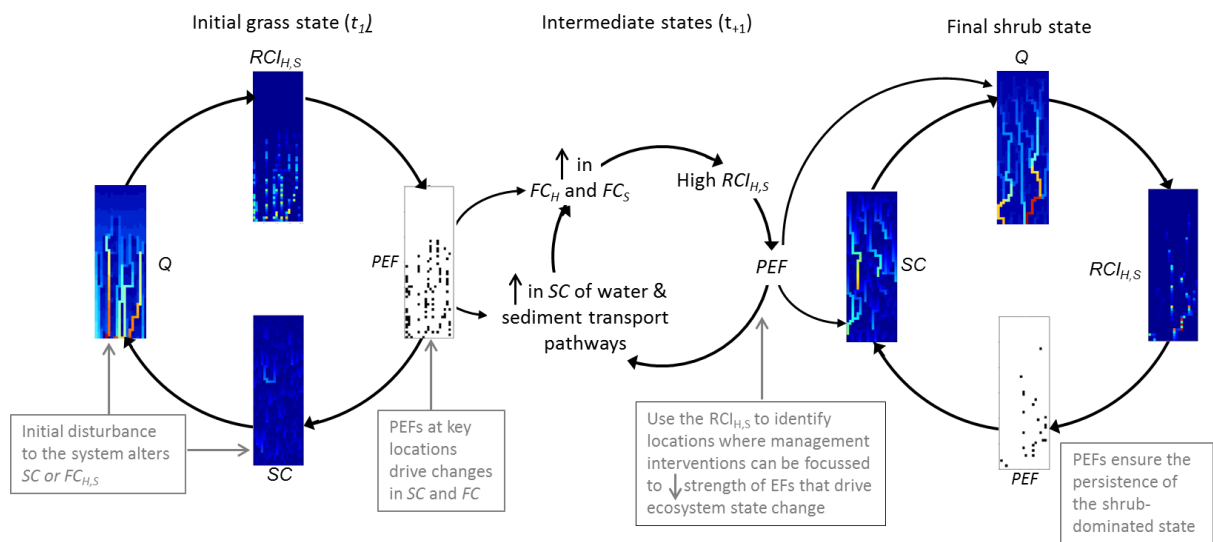


Figure 9. Conceptual model showing how structural-functional feedbacks drive changes in ecosystem state following an initial disturbance, due to pronounced ecogeomorphic feedbacks (*PEF*) occurring at specific locations within the landscape that can be identified using the $RCI_{H,S}$. Ecogeomorphic feedbacks occurring at these locations will drive changes in system structure and function with effects cascading to adjacent/downslope locations. Interventions targeted at these locations with *PEF* may provide an opportunity to halt further ecogeomorphic feedbacks and prevent a catastrophic transition to a final shrub-dominated state.